

# Identification and Characterization of Effusion Tumor Cells (ETCs) From Remnant Pleural Effusion Specimens

Yili Zhu, PhD <sup>1</sup>; Grace M. Allard, BS<sup>1</sup>; Nolan G. Ericson, BS<sup>2</sup>; Tad C. George, PhD<sup>2</sup>; Christian A. Kunder, MD, PhD<sup>1</sup>; and Alarice C. Lowe, MD <sup>1</sup>

**BACKGROUND:** Cancer is a leading cause of death worldwide, and patients may have advanced disease when diagnosed. Targeted therapies guided by molecular subtyping of cancer can benefit patients significantly. Pleural effusions are frequently observed in patients with metastatic cancer and are routinely removed for therapeutic purposes; however, effusion specimens have not been recognized as typical substrates for clinical molecular testing because of frequent low tumor cellularity. **METHODS:** Excess remnant pleural effusion samples (N = 25) from 21 patients with and without suspected malignancy were collected at Stanford Health Care between December 2019 and November 2020. Samples were processed into ThinPrep slides and underwent novel effusion tumor cell (ETC) analysis. The ETC results were compared with the original clinical diagnoses for accuracy. A subset of confirmed ETCs was further isolated and processed for molecular profiling to identify cancer driver mutations. All samples were obtained with Institutional Review Board approval. **RESULTS:** The authors established novel quantitative standards to identify ETCs and detected epithelial malignancy with 89.5% sensitivity and 100% specificity in the pleural effusion samples. Molecular profiling of confirmed ETCs (pools of 5 cells evaluated) revealed key pathogenic mutations consistent with clinical molecular findings. **CONCLUSIONS:** In this study, the authors developed a novel ETC-testing assay that detected epithelial malignancies in pleural effusions with high sensitivity and specificity. Molecular profiling of 5 ETCs showed promising concordance with the clinical molecular findings. To promote cancer subtyping and guide treatment, this ETC-testing assay will need to be validated in larger patient cohorts to facilitate integration into cytologic workflow. *Cancer Cytopathol* 2021;0:1-14. © 2021 American Cancer Society.

**KEY WORDS:** circulating tumor cells (CTCs); effusion cytology; effusion tumor cells (ETCs); epithelial malignancy detection; multiplexed immunofluorescent imaging; molecular profiling.

## INTRODUCTION

Cancer is a leading cause of death worldwide. The pathologist's role is to identify and characterize tumors to provide the appropriate diagnostic, prognostic, and predictive information for patients and their physicians. The recent development of rare tumor cell detection and capture technology facilitates the identification and characterization of malignant cells from patients' liquid biopsy specimens.<sup>1,2</sup> Circulating tumor cells (CTCs) are malignant cells that arise from the primary tumor or metastatic sites and constitute approximately 1 in a million to 1 in a billion of the nucleated cells in the peripheral blood. The presence of CTCs is significantly correlated with disease progression in patients with both localized and metastatic breast, colorectal, and prostate carcinoma.<sup>3-7</sup> Most CTC testing methods focus on tumor cells from blood, whereas there has been limited application of CTC testing methods to body fluids.<sup>8-10</sup> The expansion of CTC testing techniques to body fluid examination can contribute significantly to the field of cytology.

**Corresponding Author:** Alarice C. Lowe, MD, Pathology Department, Stanford University School of Medicine, 300 Pasteur Drive, Room H2128E, Stanford, CA, 94305 (aclowe@stanford.edu).

<sup>1</sup>Department of Pathology, Stanford University School of Medicine, Palo Alto, California; <sup>2</sup>RareCyte, Inc, Seattle, Washington

We thank the cytotechnologists from Stanford Health Care for their excellent screening, the Stanford CytoPrep Laboratory staff for technical assistance with ThinPrep slide preparation, and the patients who provided their samples for this research. We also acknowledge Guoying Liu and Chenyu Li from Paragon Genomics for their help with bioinformatic analysis (alignment, variant calling, and annotation).

**Received:** April 26, 2021; **Revised:** May 24, 2021; **Accepted:** May 25, 2021

Published online Month 00, 2021 in Wiley Online Library (wileyonlinelibrary.com)

**DOI:** 10.1002/cncy.22483, wileyonlinelibrary.com

Definitive molecular subtyping of cancer is a prerequisite for effective treatment selection and is of great importance to patients with cancer. Prevalent molecular analysis requires a moderate amount of tissue, and repeated sampling is frequently performed either for sufficient material at the time of initial diagnosis or to evaluate for the development of treatment resistance. However, tissue-based tumor profiling is frequently subject to sampling bias, and repeat sampling may subject patients to unnecessary risk. Thus the integration of other testing materials, such as blood and other body fluids (pleural effusions, cerebrospinal fluid, urine, and saliva, etc) for molecular profiling can facilitate cancer subtyping.<sup>11,12</sup>

Malignant pleural effusions, which frequently are observed in patients with metastatic lung adenocarcinoma (ACA), may serve as a new source of profiling material. Patients who have lung ACA frequently present with advanced local disease or distant metastasis. Despite the poor prognosis of advanced lung cancer, with a low 5-year survival rate (4%-15%),<sup>13-15</sup> targeted therapies in appropriately selected patients have shown significant survival benefits.<sup>16,17</sup> Malignant pleural effusions present in patients with metastatic lung ACA are routinely drained and removed for therapeutic purposes.<sup>18</sup> Malignant pleural effusions have not yet been recognized as routine substrates for the cytologic or molecular testing pipeline because of their frequent low tumor fraction and sparse cellularity.<sup>19-21</sup>

In this study, we modified and applied a CTC testing method to examine malignancies from pleural effusion specimens with high sensitivity. We first established quantitative criteria to faithfully distinguish tumor cells from the background cells. These criteria were validated in pleural effusion samples and used to identify effusion tumor cells (ETCs) from 21 patients. By using this novel ETC testing method, we detected malignancy in patients with high sensitivity and specificity. Further molecular profiling of a subset of confirmed ETCs revealed key pathogenic mutations that also were identified in blinded concurrent or prior clinical molecular testing.

## MATERIALS AND METHODS

### *Cell Line Controls and Sample Collection and Preparation*

For control blood samples, model cancer cells (BT474, breast ductal carcinoma cell line; ATCC HTB-20) were

mixed with healthy blood samples and fixed with a proprietary preservative to preserve cell integrity and density. The spike-in blood samples were processed using the AccuCyte sample preparation system (RareCyte Inc) to isolate nucleated cells and spread them evenly onto SuperFrost Plus Microscope Slides (Fisherbrand). The slides were air-dried and stored at  $-20^{\circ}\text{C}$ .

All cytologic samples were obtained with Institutional Review Board approval. We collected remnant ThinPrep (TP) vials from samples preliminarily screened as suspicious or positive for malignancy by a cytotechnologist or samples screened as negative from December 2019 to November 2020 at Stanford Health Care. Effusion samples were collected into TP vials supplied with PreservCyt solution and stored at room temperature without additional prefixation treatments. Each remnant TP vial contained 10 to 25 mL of material with sparse to dense cellularity and were used to generate 2 to 4 TP slides using the Hologic ThinPrep 2000 Processor (Hologic, Inc) by the Stanford Cytology Laboratory. The TP slides were air-dried at room temperature and stained immediately or within 72 hours (stored at  $-20^{\circ}\text{C}$ ).

### *Multiplexed Immunofluorescent Imaging Workflow*

We performed multiplexed fluorescent staining of the blood-sample control slides and TP slides using a custom RarePlex Staining Kit (RareCyte Inc). Briefly, the air-dried slides were fixed in 10% neutralized buffered formalin for 10 minutes and then blocked with 10% goat serum. The blocked slides were next subjected to the RarePlex Staining Kit and incubated sequentially with different RarePlex reagents in the dark. The slides were mounted with mounting media and coverslipped with imaging coverslips (Fisher Scientific). The slides were scanned at  $\times 10$  magnification using the CyteFinder II HT Instrument (RareCyte Inc). Four-channel images were captured using a consistent configuration (nucleus: 405 nm, 0.005 msec; cytokeratin [CK]: 488 nm, 0.1 msec; CD45: 555 nm, 0.1 msec; epithelial cell adhesion molecule [EpCAM]: 647 nm, 0.1 msec) for all TP slides. The preliminary ETC candidates were screened and ranked using the integrated machine-learning algorithm<sup>22</sup> in CyteMapper software (RareCyte Inc). ETCs were further visually confirmed and enumerated by trained reviewers.

### **Development of Standards for CTC and ETC**

We first studied the CTCs from BT474 cell spike-in blood samples following a consistent staining and imaging protocol. After reviewing hundreds of model cancer cells, we found that the malignant cells generally displayed strong CK staining, strong EpCAM staining, and weak CD45 staining compared with the white blood cells (WBCs) in the background. To best evaluate the staining levels, we measured the mean fluorescent intensity (MFI) for each biomarker in a group of cells.

To calculate the MFI values, we first defined the outline of a tumor cell or WBC. During image analysis, each pixel has 1 intensity reading, which reflects the strength of fluorescent signal in this pixel. We measured the total fluorescent intensity of the cell (sum of intensity readings from each pixel enclosed in the cell), divided it by the number of pixels included in the cell, and derived the raw MFI values. The background fluorescent intensity was further subtracted from raw MFI values to remove the potential influence of uneven background staining. After comparing the MFI values between a group of tumor cells ( $N = 80$ ) and WBCs ( $N = 50$ ), we set tentative cutoffs for positive tumor cells at an EpCAM MFI value  $> 100$  arbitrary units (au), a CK MFI value  $> 500$  au, and a CD45 MFI value  $< 100$  au. WBCs displayed MFI values of CD45  $> 100$  au, EpCAM  $< 100$  au, and CK  $< 100$  au.

We next examined a pilot group of positive ETCs, confirmed by a cytopathologist (A.C.L.), following the same analysis protocol. We found that the tentative cutoffs for EpCAM and CD45 in the CTCs still held true for the ETCs; however, the CK MFI values varied dramatically in ETCs. We thus applied only the EpCAM and CD45 cutoffs for ETC determination in all 25 samples. The hematopoietic cells from patient effusion samples displayed a staining pattern identical to that of the WBCs from the blood samples. In addition, mesothelial cells were observed as a significant background population in effusion specimens and showed a consistent MFI staining pattern of CK  $> 100$  au, CD45  $< 100$  au, and EpCAM  $< 100$  au.

### **ETC Isolation and Library Preparation**

To obtain high-quality ETC libraries, we selected 5 representative patient samples from the recently processed samples. The previously examined immunofluorescent-stained patient slides with confirmed ETCs were incubated at 37 °C in 1 × phosphate-buffered saline to

remove coverslips and then placed in a CyteFinder II HT Instrument for semiautomated single-cell retrieval with the integrated CytePicker Retrieval Module. Coordinates of confirmed ETCs were imported from CyteFinder scan files, followed by mechanical retrieval, as described previously.<sup>22,23</sup> Cells were deposited into low-binding polymerase chain reaction tubes (Axygen), confirmed visually, and stored at  $-80$  °C. Each sample pool was comprised of 5 picking events, and each picking event collected either a single cell or a small cell cluster. Five sample pools were collected per patient, and 3 of the 5 pools were subjected to library preparation.

To generate library preparations, cells were thawed briefly on ice, followed by the addition of Single Cell Lysis Buffer (Takara Bio) and room temperature incubation for 1 hour. Cell lysate was used as the template for the CleanPlex OncoZoom Cancer Hotspot Panel (Paragon Genomics). Library DNA concentrations were measured with the Qubit dsDNA HS Assay Kit (Thermo Fisher Scientific), and fragment size distribution was measured using the Bioanalyzer High Sensitivity DNA Kit (Agilent). Libraries were mixed in equimolar ratios, and sequencing was performed on an Illumina MiSeq with MiSeq Reagent Kit version 2 (300-cycle) cartridges.

### **Next-Generation Sequencing Data Analysis and ETC Pool Variant Analysis**

The Paragon Genomics OncoZoom panel consists of 601 amplicons and was designed to interrogate common mutations in 65 cancer-related genes. Raw sequencing reads were trimmed for adaptors using software cutadapt (<https://github.com/marcelm/cutadapt>). The sequences were then mapped to the human reference genome GRCh37/hg19 with bwa-mem using the Sentieon analysis package (Sentieon, Inc). Subsequent indel re-alignment and base quality recalibration were also accomplished with the Sentieon package. Mapped reads were filtered, and only reads in which start positions matched amplicon start positions were kept. Amplicon read depth uniformity, mapping rate, on-target rate, and primer-dimer content were surveyed and used to assess library quality. Variant calling was performed using Vardict<sup>24</sup> with the amplicon mode. Called variants were filtered, and those with  $\geq 100$  read coverage and allele frequency  $> 1\%$  were kept. Variants were counted as somatic mutations for a given patient if they: 1) were reported in COSMIC

database v71,<sup>25</sup> and 2) were present in  $\geq 2$  samples potentially containing cancer cells/DNA at a minimum allele frequency of 1%. We cross-referenced prevalence databases (genome aggregation, gnomAD\_exon) to identify single nucleotide variants. The variants with a global mean allele frequency  $>0.1\%$  were considered likely germline and were not further considered in this study. The ETC variant results were subsequently compared with the electronic medical record (with Institutional Review Board approval) at Stanford and were discussed to confirm the somatic mutations in the patient samples.

### Data Analysis

All patient information, including patient age, sex, cancer history, and the cellularity information from 11 cases, was collected from the electronic medical record with Institutional Review Board approval. Statistical significance was determined using a Student *t* test on unpaired data with unequal variance, and  $P < .0001$  was considered statistically significant.

## RESULTS

### General Patient Information

Twenty-five pleural effusion remnant specimens determined to be positive or negative for malignancy on final cytology were collected from 21 patients from December 2019 to November 2020. The cohort consisted of 11 women and 10 men, and the average age was  $66.1 \pm 15.1$  years (range, 26-98 years). As shown in Table 1, the current or prior diagnoses of the patients included 12 lung ACAs, 1 colorectal carcinoma, 1 small cell neuroendocrine carcinoma, 1 triple-negative breast carcinoma, 1 mesothelioma, 1 metastatic thymoma, 1 clinically localized thymoma, 1 large B-cell lymphoma, and 2 with no known history of malignancy. The identification and counting of ETCs in this study were performed with the patient diagnoses blinded.

### Development and Validation of Quantitative Tumor Cell Standards

Because no quantitative criteria existed to define tumor cells in patient samples, we first sought to establish consistent standards to faithfully distinguish tumor cells from other background cells based on their multiplex staining patterns. We started by examining the control samples with model cancer cells (BT474, breast ductal

**TABLE 1.** Patient Information

Patient	Age, y	Sex	Type of Cancer
1 <sup>a</sup>	68	Woman	Lung adenocarcinoma
2	98	Woman	Lung adenocarcinoma
3	69	Man	Lung adenocarcinoma
4	72	Woman	Lung adenocarcinoma
5 <sup>a</sup>	57	Man	Lung adenocarcinoma
6 <sup>a</sup>	75	Man	Lung adenocarcinoma
7	70	Man	Lung adenocarcinoma
8	41	Man	Lung adenocarcinoma
9	80	Woman	Lung adenocarcinoma
10	71	Man	Lung adenocarcinoma
11	78	Man	Lung adenocarcinoma
12	68	Woman	Lung adenocarcinoma
13	79	Woman	Mesothelioma
14	55	Woman	Colorectal carcinoma
15	63	Woman	Small cell carcinoma
16	70	Woman	Triple-negative breast carcinoma
17	65	Woman	Metastatic thymoma
18 <sup>b</sup>	46	Man	Thymoma (not metastatic)
19	70	Man	No malignant history
20	68	Man	No malignant history
21	26	Woman	Large B-cell lymphoma

<sup>a</sup>These patients contributed bilateral pleural effusion specimens.

<sup>b</sup>This patient contributed 2 ipsilateral pleural effusion specimens taken 56 days apart.

carcinoma cell line; ATCC HTB-20) spiked into healthy blood samples (Fig. 1A). The 3 biomarkers we chose for multiplex staining pattern analysis were CK cocktail (epithelial marker), CD45 (WBC marker), and EpCAM (epithelial marker). After reviewing hundreds of cancer cells and WBCs, we found that the tumor cells consistently displayed strong CK, strong EpCAM, and weak CD45 staining compared with the WBCs in the background, which displayed weak CK, weak EpCAM, and strong CD45 staining (Fig. 1B). To determine a numeric threshold to separate *strong staining* from *weak staining* for each biomarker, we quantitatively examined and compared whole-cell MFI values, as described above (see Materials and Methods), between representative tumor cells and WBCs. As depicted in Figure 1C, tumor cells ( $N = 80$ ), compared with WBCs ( $N = 50$ ), exhibited a significantly higher mean CK MFI value ( $654.0 \pm 52.8$  vs  $11.2 \pm 1.1$  au;  $P < .0001$ ) and mean EpCAM MFI value ( $140.4 \pm 7.5$  vs  $2.1 \pm 0.3$  au;  $P < .0001$ ) while displaying a significantly lower mean CD45 MFI value than the WBCs ( $16.5 \pm 1.5$  vs  $201.9 \pm 21.6$  au;  $P < .0001$ ). Based on the explicit and distinct pattern of tumor cells, we set tentative cutoffs to define tumor cells as any given cell exhibiting a CK MFI value  $>500$ , an EpCAM MFI value  $>100$ , and a CD45 MFI value  $<100$  au.

Next, we sought to validate the cutoffs of model cancer cells in tumor cells from pleural effusion samples

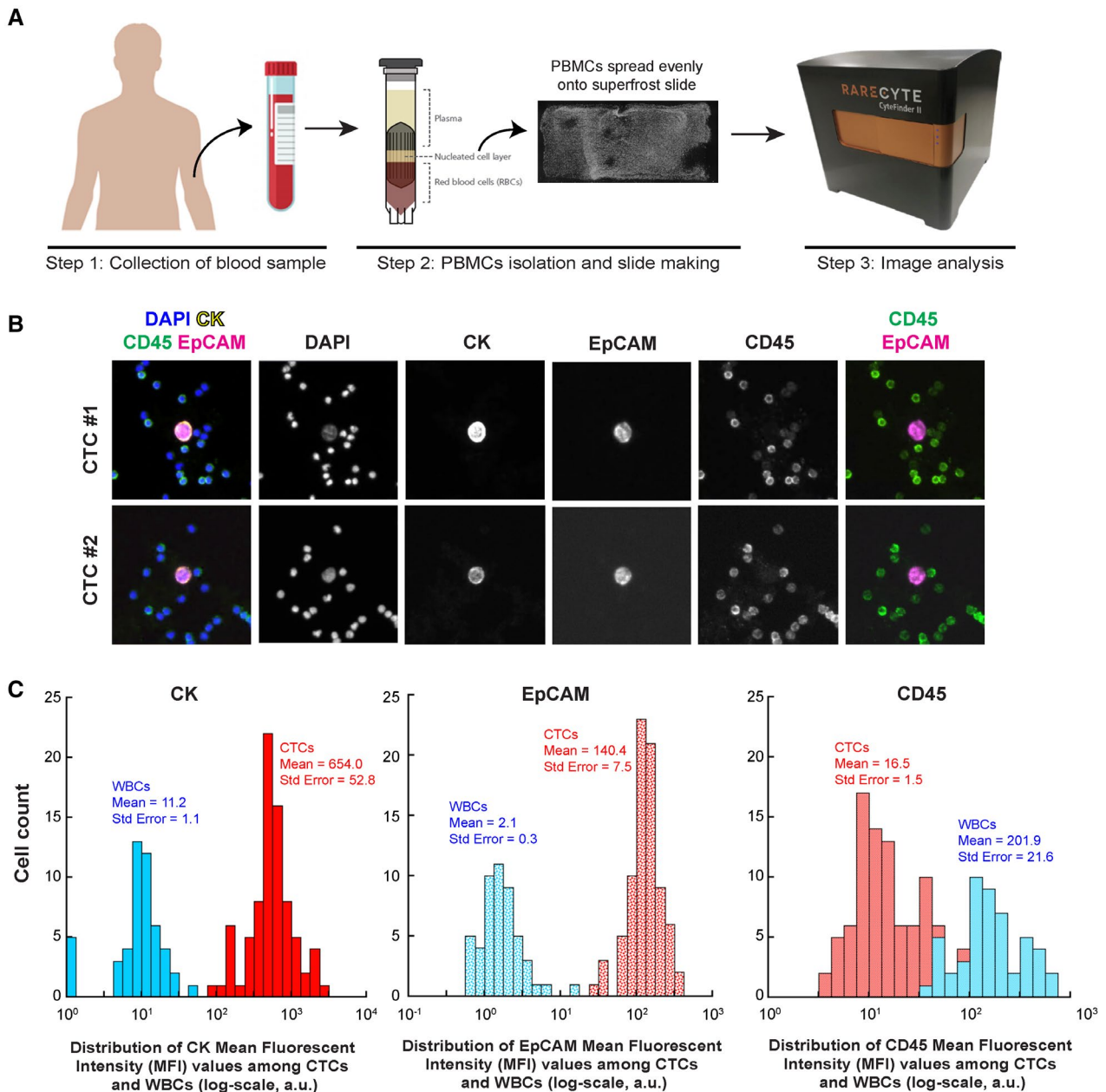


**Figure 1.** The establishment of a quantitative standard for circulating tumor cells (CTCs) identification. (A) This schematic depicts blood sample processing and CTC imaging workflow. PBMCs indicates peripheral blood mononucleated cells. (B) Representative 4-channel immunofluorescent images of single CTCs and background white blood cells (WBCs) are shown. (C) This log-scale histogram depicts the mean fluorescent intensity (MFI) value distribution of each indicated biomarker in CTCs ( $N = 80$ ) and WBCs ( $N = 50$ ). CTCs and WBCs exhibited opposite staining patterns in the cytokeratin (CK), epithelial cell adhesion molecule (EpCAM), and CD45 channels. a.u. indicates arbitrary units; Std Error, standard error.

by examining a pilot group of ETCs. TP slides were prepared using the remnant pleural effusion material from 3 patients with lung ACA (patients 1, 3, and 4). The TP slides were stained and imaged following the same protocol (Fig. 2A). The ETC candidates ( $N = 66$ ) were screened, identified, and confirmed by a cytopathologist.

We examined the MFI values of CK, EpCAM, and CD45 in those confirmed ETCs, and distribution of MFI values of each biomarker is plotted in Figure 2C. Similar to the patterns shown in model tumor cells (shown in Fig. 1), all confirmed ETCs exhibited an EpCAM MFI value  $>100$  au ( $213.6 \pm 15.3$  au) and a CD45 MFI value

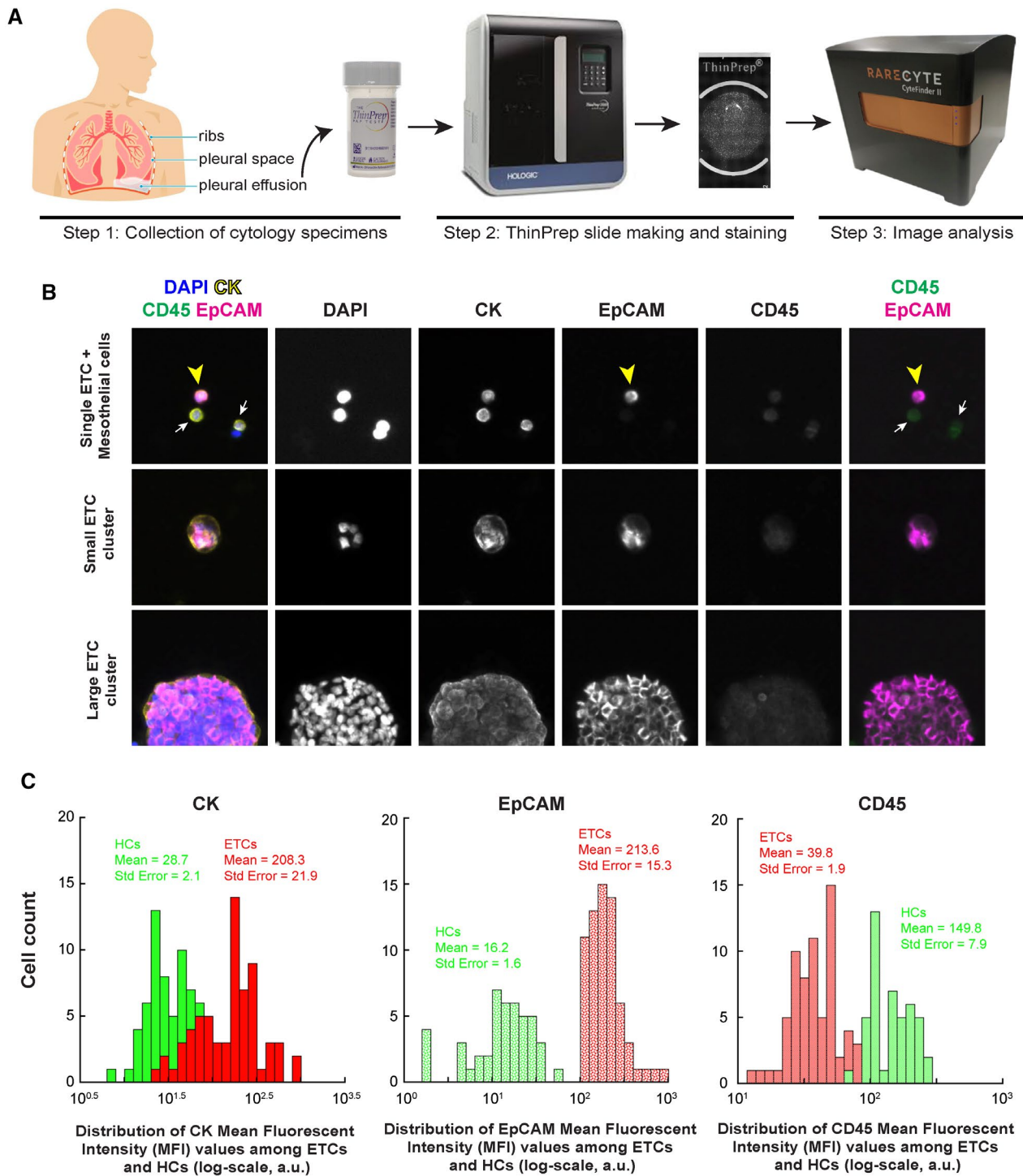


**Figure 2.** Validation of effusion tumor cell (ETC) quantitative standards in a pilot group of pleural effusion samples. (A) This schematic depicts ThinPrep processing and ETC imaging workflow. (B) Representative 4-channel fluorescent images of single ETCs, a small ETC cluster, and a large ETC cluster are shown. Yellow arrowheads indicate a single ETC, and white arrows indicate mesothelial cells. (C) This log-scale histogram depicts the mean fluorescent intensity (MFI) value distribution of each indicated biomarker in both ETCs (N = 66) and hematopoietic cells (HCs) (N = 45). ETCs and HCs showed minimal overlapping staining patterns in cytokeatin (CK), epithelial cell adhesion molecule (EpCAM), and CD45 channels. a.u. indicates arbitrary units; Std Error, standard error.

<100 au ( $39.8 \pm 1.9$  au). However, the CK MFI values of confirmed ETCs varied significantly, with an average MFI value of  $208.3 \pm 21.9$  au (<500 au). In contrast, the hematopoietic cells present in pleural effusion samples showed strong CD45 staining ( $149.8 \pm 7.9$  au), with only base-level EpCAM staining ( $16.2 \pm 1.6$  au) and CK staining ( $28.7 \pm 2.1$  au) (Fig. 2C). On the basis of these findings, we validated that the cutoffs for EpCAM and CD45 were still applicable in pleural effusion samples for ETC identification, whereas the CK cutoff was removed due to its variability.

### **Comparison of ETC Results to Original Clinical Diagnosis**

By using the validated MFI value cutoffs for EpCAM and CD45, we successfully separated ETCs from the background cells in many patients. The background cells observed in pleural effusion samples were more diverse and differed significantly from those present in the control spike-in blood samples. The background cells included mesothelial cells, histiocytes, lymphocytes, neutrophils, and other inflammatory cells, and background material included acellular debris. Among all these nontumor cells, mesothelial cells displayed the most similar pattern to ETCs in CK and CD45 staining, but not in EpCAM staining (Fig. 2B, white arrows). As shown in Figure 3A, we quantified 60 mesothelial cells from different patients and demonstrated that mesothelial cells consistently displayed only base-level staining of CD45 and EpCAM (CD45:  $23.3 \pm 1.2$  au; EpCAM:  $39.7 \pm 2.7$  au), whereas the CK staining varied significantly ( $209.5 \pm 20.6$  au).

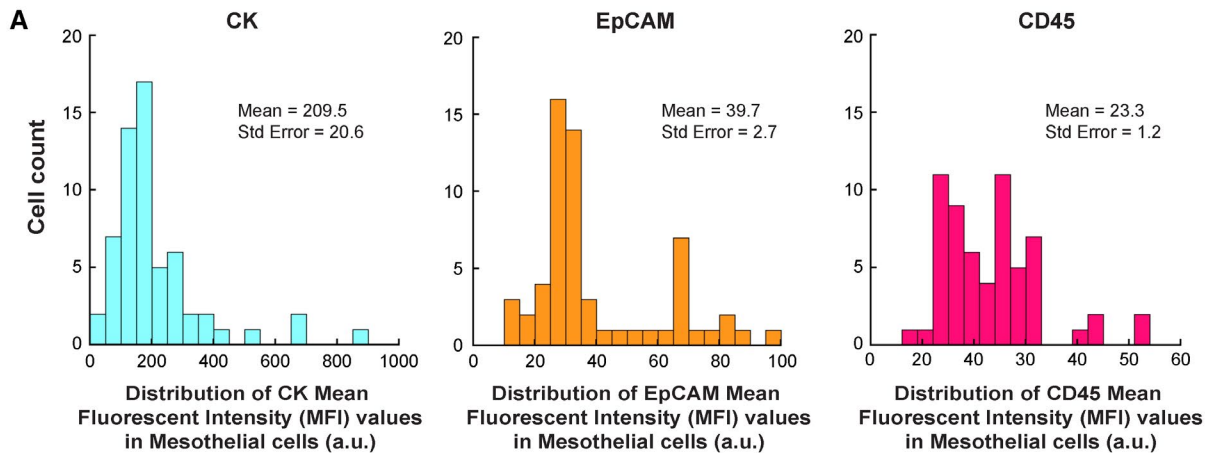
The ETCs identified in the effusion specimens were observed in the form of either single cells or clusters (Fig. 2B) with a sparse-to-abundant cellularity. To better report ETC numbers, we classified the ETCs into 3 different groups: 1) a single ETC (an individual ETC), 2) a small cluster (2-10 ETCs), and 3) a large cluster (>10 ETCs). ETCs from 2 or 3 parallel TP slides were examined for each patient by 2 independent qualified researchers to verify numerical accuracy. The frequency of each ETC cluster type is summarized in Table 2 for all 25 samples from 21 patients. Our ETC testing methodology identified malignant cells in patients with different cancer types and detected positive ETC results in 17 confirmed malignant samples, but not in the other 2 malignant samples (Table 2). Overall, our ETC testing showed high sensitivity (89.5%; 17 of 19 samples) and specificity (100%; 6 of

6 samples) for identifying malignancy compared with the clinical diagnosis (Fig. 3B).

Furthermore, our ETC results showed a promising correlation with the reported cell block tumor cellularity (available in 11 patients). When ranking the 11 patient samples with reported tumor cellularity from low to high, our ETC results showed a similar increasing trend in ETC numbers. As summarized in Table 2 and Figure 3C, sample 2 was reported with 0% cell block tumor cellularity, and we identified 0 ETCs and 0 clusters in this effusion sample. For the 4 malignant patient samples (samples 4, 10, 11, and 14) with reported 5% to 20% tumor cellularity, we detected a moderate number of ETCs in all 4 samples (mean: 76.3 single cells, 40.3 small clusters, and 27 large clusters). For the remaining 6 samples reported to have >20% tumor cellularity (samples 1A, 3, 5A, 6B, 9, and 12), we detected a large amount of ETCs and clusters in 5 of 6 samples (mean: 264.8 single cells, 77 small clusters, and 192 large clusters). Taken together, our ETC results showed high sensitivity and specificity in detecting malignancy in remnant pleural effusion specimens of small volume and reflected the tumor cellularity reported in the clinical samples.

### **Molecular Profiling of Single ETCs Revealed Key Pathogenic Mutations**

To further obtain cancer subtyping information from confirmed ETCs, we collected ETCs (5 cells or small clusters per sample) from 4 malignant patient samples (patients 9, 10, 12, and 16) and collected CD45-positive cells from patient sample 18A as a control. We lysed the cell samples and performed library preparations on  $\geq 4$  samples per patient using the OncoZoom Panel Kit (covering 601 amplicons in 65 genes). After quality-control examination of library DNA concentrations and fragment sizes, the 3 libraries of the best quality from each patient were combined and sequenced on an Illumina MiSeq machine. To ensure that our 5-cell profiling protocol was working properly, we first validated this workflow using model cancer cells. For the ETC molecular profiling, we managed to retrieve high-quality sequencing results with great coverage uniformity (80%-90%; coverage uniformity = percentage of targeted base positions in which the read depth is >0.2 times the mean region target coverage depth) for most samples (samples 10, 12, 16, and 18A). Because of its extremely low library DNA concentration, sample 9 showed a significantly lower uniformity



**B**

Sample No.	Clinical cytology diagnosis	ETC findings
1-15	All 15 cases diagnosed with lung adenocarcinoma (ACA)	positive ETC results detected in <b>13</b> cases
16-19	1 colorectal carcinoma, 1 neuroendocrine carcinoma, 1 triple-negative breast carcinoma, 1 mesothelioma	positive ETC results detected in all <b>4</b> cases, with 1 case diagnosed with mesothelioma
20-25	All 6 cases were diagnosed negative for malignancy	negative ETC results for all <b>6</b> cases

**ETC testing: 89.5% sensitivity (17 of 19) ; 100% specificity (6 of 6)**

**C**

Tumor cellularity (%)	Reported case number	ETC results for according cases
0%	1	1 of 1 case with zero ETCs: 0 single cell, 0 small cluster, 0 large cluster
5-20%	4	4 of 4 case with medium number of ETCs: 76.3 single cells, 40.3 small clusters, 27 large clusters
>20%	6	5 of 6 case with high number of ETCs: 264.8 single cells, 77 small clusters, 192 large clusters

**Figure 3.** Examination of mesothelial cell staining patterns and comparison between effusion tumor cell (ETC) results and original clinical findings. (A) This histogram depicts the mean fluorescent intensity (MFI) value distribution of each indicated biomarker in mesothelial cells (N = 60). Mesothelial cells showed variable MFI in the cytokeratin (CK) channel and base-level staining in the epithelial cell adhesion molecule (EpCAM) and CD45 channels. (B) This summary table depicts the correlation between the current ETC results and clinical cytology findings in detecting epithelial malignancy in all 21 patients. (C) This summary table reveals a concordance between the ETC numbers and cell block tumor cellularity in 11 patients. a.u. indicates arbitrary units; Std Error, standard error.

**TABLE 2.** Effusion Tumor Cell Results From Each Sample in This Study

Case <sup>a</sup>	Single ETCs	ETC Small Clusters (2-10 ETCs)	ETC Large Clusters (>10 ETCs)	Cell Block Tumor Cellularity, %	Summary of Original Clinical Diagnosis
1A	1	3	2	Not Reported	Metastatic adenocarcinoma: The cytologic preparations are cellular with malignant clusters. The cell block sections show mostly blood and mesothelial cells.
1B	37	66	184	30	Metastatic adenocarcinoma: Both cytologic preparations and cell block sections are cellular with malignant clusters and single cells.
2	0	0	0	0	Metastatic adenocarcinoma: The cytologic preparations are moderately cellular, containing malignant glandular cells in small clusters and single cells. The cell block section findings are noncontributory.
3	368	86	37	90	Metastatic adenocarcinoma: The cytologic preparations and cell block sections contain numerous clusters of malignant glandular cells, indicative of metastatic adenocarcinoma.
4	89	68	52	10	Metastatic adenocarcinoma: The cytologic preparations and cell block sections show malignant glandular epithelial cells in cohesive clusters and single dispersed cells.
5A	723	120	125	>80	Metastatic adenocarcinoma: The cytologic preparations and cell block sections are cellular, containing numerous malignant glandular epithelial cells arranged in clusters and single cells.
5B	428	107	1232	Not reported	Metastatic adenocarcinoma: The cytologic preparations and cell block sections are cellular, containing numerous malignant glandular epithelial cells arranged in clusters and single cells.
6A	1	0	0	Not reported	Malignant: The cytologic preparations and cell block sections show a population of malignant epithelioid cells arranged in small, cohesive clusters and as single dispersed cells.
6B	3	0	0	70	Malignant: The cytologic preparations and cell block sections show malignant epithelioid cells arranged in small clusters and single cells. On immunohistochemical staining, the malignant cells are positive for MOC31. Calretinin is negative in the malignant cells and highlights background mesothelial cells. Together, the findings support involvement by metastatic carcinoma.
7	0	0	0	Not reported	Metastatic adenocarcinoma: The cytologic preparations and cell block sections demonstrate various involvement by malignant glandular epithelial cells presenting in cohesive clusters and as single dispersed cells.
8	3	0	0	Not reported	Metastatic adenocarcinoma: The cytologic preparations are cellular, containing malignant glandular cells in 3-dimensional clusters and single cells. The cell block sections are scanty cellular but show concordant features.
9 <sup>b</sup>	123	44	4	90	Metastatic adenocarcinoma: The cytologic preparations and cell block sections are abundantly cellular and show malignant epithelial cells in cohesive clusters and single dispersed cells. Immunohistochemical stains show that the malignant cells are focally positive for BER-EP4 and extensively positive for TTF-1. Calretinin highlights scattered mesothelial cells. These findings support metastatic adenocarcinoma, consistent with lung origin.
10 <sup>b</sup>	92	68	25	Approx 5	Malignant: The cytologic preparations and cell block sections are moderately cellular and show a population of variously cohesive cells with enlarged, pleomorphic nuclei, nuclear contour irregularities, prominent nucleoli, multinucleation, and moderate-to-abundant amounts of delicate, occasionally vacuolated cytoplasm. Immunohistochemistry shows that these cells are positive for MOC31, consistent with metastatic carcinoma.
11	4	13	31	10	Metastatic adenocarcinoma: The cytologic preparation and cell block sections contain malignant epithelial cells arranged in clusters and single cells. The cells demonstrate moderate amounts of finely vacuolated cytoplasm and enlarged hyperchromatic nuclei with prominent nucleoli. These cytologic features are indicative of a metastatic adenocarcinoma.
12 <sup>b</sup>	73	69	610	80	Metastatic carcinoma: The cytologic preparations and cell block sections are abundantly cellular and show malignant epithelial cells in cohesive clusters and single dispersed cells.
13	152	520	659	Not reported	Malignant: The cytologic preparations and cell block sections are cellular, showing malignant epithelioid cells appearing in cohesive clusters and as single dispersed cells. The cells exhibit enlarged, irregular nuclei, visible nucleoli, and a moderate amount of vacuolated cytoplasm. Together with the patient's history (prior cytology reviewed in comparison), the findings are consistent with involvement by mesothelioma.

TABLE 2. Continued

Case <sup>a</sup>	Single ETCs	ETC Small Clusters (2-10 ETCs)	ETC Large Clusters (>10 ETCs)	Cell Block Tumor Cellularity, %	Summary of Original Clinical Diagnosis
14	120	12	0	<5	Metastatic adenocarcinoma: The cytologic preparations and cell block sections contain clusters of malignant epithelial cells with enlarged and irregular nuclei and delicate vacuolated cytoplasm. These cytologic features are diagnostic for metastatic adenocarcinoma.
15	29	22	156	Not reported	The cytologic preparations and cell block sections are cellular and show clusters of malignant cells with high nucleus-to-cytoplasmic ratios, nuclear molding, coarse chromatin, and scant delicate cytoplasm. On immunohistochemistry, these cells express TTF-1 and synaptophysin and are negative for CK7, CK20, and calretinin. Overall, the morphologic and immunophenotypic findings are diagnostic of metastatic neuroendocrine carcinoma.
16 <sup>b</sup>	68	58	95	Not reported	Metastatic adenocarcinoma: The cytologic preparations and cell block sections are abundantly cellular and show malignant epithelial cells in cohesive clusters and single dispersed cells. The morphologic findings are those of metastatic adenocarcinoma and are consistent with a breast primary.
17	0	0	0	NA	Negative for malignancy
18A <sup>b</sup>	0	0	0	NA	Negative for malignancy: The cytologic preparations and cell block sections show predominantly mesothelial cells, histiocytes, and lymphocytes; a single cohesive cluster of atypical epithelioid-to-spindled cells with oval nuclei is identified (slide A2). Although this cluster raises the possibility of involvement by an epithelial process, the cells of interest are not present on multiple cell blocks (A1 and A2) for further evaluation. By immunohistochemistry performed on blocks A1 and A2, calretinin highlights mesothelial cells, whereas Pax8 highlights background lymphocytes, and p63 is negative. Overall, there is no definitive evidence of involvement by the patient's thymic neoplasm. Clinical and imaging correlation is recommended. If the fluid re-accumulates, further sampling may be considered.
18B	0	0	0	NA	Negative for malignancy
19	0	0	0	NA	Negative for malignancy
20	0	0	0	NA	Negative for malignancy
21	0	0	0	NA	Negative for malignancy

Abbreviations: Approx, approximately; ETCs, effusion tumor cells; NA, not applicable.

<sup>a</sup>"A" and "B" indicate different samples from the same patient collected either from contralateral sites or from the same site on different days.

<sup>b</sup>These patients were selected for molecular profiling.

compared with the other samples (Fig. 4A). Our profiling results revealed several interesting point mutations in each patient sample.

In patient 9 (Fig. 4B), we detected a point mutation in *TP53* (*I162F*; 49%) from the 5 cells. By comparison, the clinical molecular testing based on the Stanford Solid Tumor Actionable Mutation Panel (STAMP) (covering 130 genes) performed on the same effusion sample reported mutations in *EGFR* (*L858R*; 97%; pathogenic) and *TP53* (*I162F*; 37%; likely pathogenic). Our assay successfully detected the *TP53* (*I162F*) mutation; however, it missed the pathogenic *EGFR* (*L858R*) point mutation. *CDK4* was not included in the OncoZoom panel (65 genes) and thus was beyond the scope of our current testing panel.

For patient 10 (Fig. 4C), our profiling results showed a mutation in *KRAS* (*G12A*; 83%), whereas the clinical results obtained from a prior lung fine-needle

aspiration specimen showed mutations in *KRAS* (*G12A*; 8%; pathogenic), *KEAP1* (*E441X*; 10%; likely pathogenic), and *STK11* (*I26fs*; likely pathogenic). Our profiling assay identified the main pathogenic mutation *KRAS* (*G12A*) with significantly higher variant allele fractions (83% vs 8%); however, it did not detect the likely pathogenic mutation in *STK11*. This could be because the *STK11* (*I26fs*) mutation was subclonal and was not present in the 5 cells we selected for sequencing. *KEAP1* was not included in our current OncoZoom panel and thus was beyond the detection scope of our assay.

The 5-cell profiling results of patient 12 (Fig. 4D) revealed mutations in *ERBB2* (*S310F*; 92%) and *PTEN* (*P213fs*; 86.8%) and an *EGFR* exon 19 deletion (42%), all of which were also reported as pathogenic mutations in clinical testing. The clinical STAMP assay performed on the same sample reported an additional frame-shift

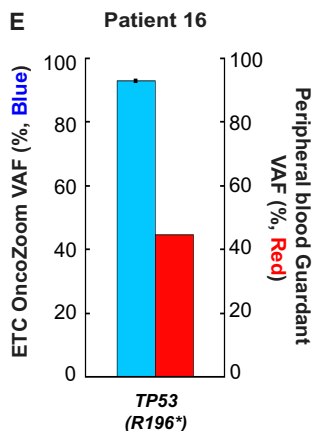
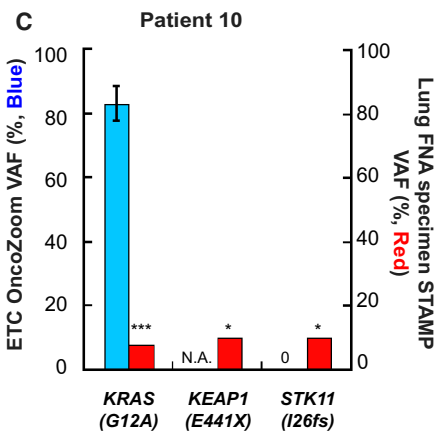
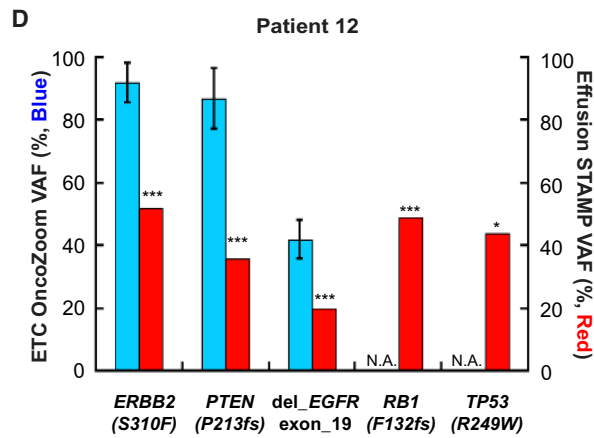
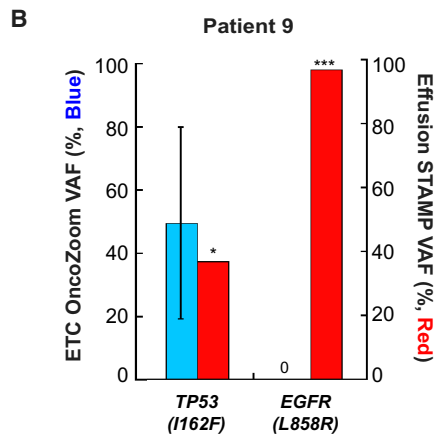
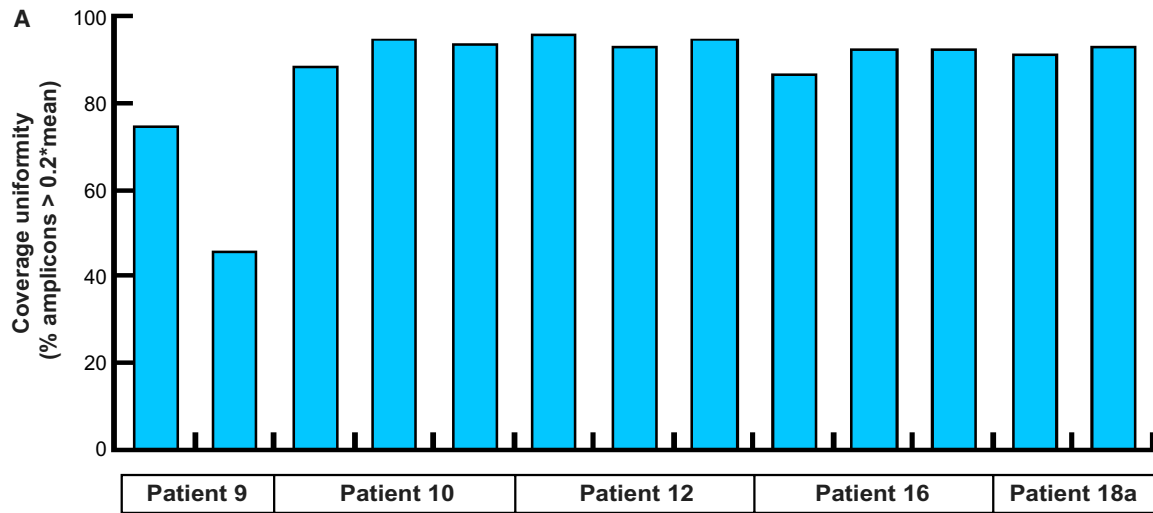


Figure 4F is a table showing ETC per-variant sensitivity for four patients.

	ETC per-variant sensitivity (%)
Patient 9	50
Patient 10	33.3
Patient 12	60
Patient 16	100

**Figure 4.** Molecular profiling of selected patient effusion tumor cells (ETCs) (5 cells) revealed key mutations supported by clinical reports. (A) This plot shows the coverage uniformity (%amplicons > 0.2\*mean) in each library prepared using ETCs from 5 selected patients. (B-E) Summary plots depict side-by-side comparisons in point mutations identified from each indicated patient between our ETC assay (blue) and clinical testing (red). (F) This table depicts the per-variant sensitivity of profiling results in from 4 patients with malignant disease: per-variant sensitivity = (no. of confirmed somatic mutations identified in ETC assay)/(no. of identified somatic mutations in the Stanford Solid Tumor Actionable Mutation Panel [STAMP] assay). Error bars represent the standard error (Std Error). Pathogenic mutations (3 asterisks) and likely pathogenic mutations (1 asterisk) are indicated. N.A. indicates mutations that were not covered in the OncoZoom panel; VAF, variant allele frequency.

mutation in *RBI* (*F132fs*; pathogenic) and a point mutation in *TP53* (*R249W*; likely pathogenic); however, these 2 targets fell out of the detection scope of our testing panel.

Finally, our molecular profiling of patient 16 (Fig. 4E) displayed a deleterious mutation in *TP53* (*R196\**; 93%), which was identified in clinical testing as a pathogenic mutation (based on the Guardant 360 results, performed on a peripheral blood sample). For the benign patient sample 18A, we only detected likely germline variants.

Overall, our 5-ETC profiling assay showed promising results in identifying the key pathogenic mutations driving cancer and high per-variant sensitivity in many samples (Fig. 4F). However, our current profiling panel will need to be further expanded to provide comprehensive molecular profiling information.

## DISCUSSION

In this study, we examined the tumor cells present on TP slides prepared using excess remnant pleural effusion samples of small volume (10-25 mL from each TP container, which is significantly smaller than the recommended 50-75 mL sample for diagnostic adequacy)<sup>26</sup> and managed to detect malignancy from a small pool of cells (as few as 1000 total cells). We have also established a consistent and quantitative standard for ETC identification, which worked well for most patients with carcinoma in this study. Our novel ETC-testing assay detected tumor cells from different primary sites with high sensitivity and specificity. Furthermore, we successfully isolated and performed genetic analysis of the confirmed ETCs (5 cells per sample) in selected patients using targeted next-generation sequencing methods and revealed key pathogenic mutations in patients that overlapped largely with the clinical molecular testing results.

However, we noticed that our current ETC-testing assay failed to detect malignancy in 2 samples diagnosed as lung ACA (lung ACA; patients 2 and 7). In addition, in sample 6B, with reported high tumor cellularity (lung ACA; 70% tumor cellularity), we only identified 3 single ETCs and zero ETC clusters from a pool of 1251 cells (Table 2), which is significantly lower than the number of single ETCs and clusters present in other patients with comparable tumor cellularity. This possibly may be attributed to the absence of malignant cells and clusters in the remnant effusion samples or to an

unequal distribution of cells (sampling error). For future directions, we seek to improve the performance of our current multiplexed immunofluorescent staining panel by incorporating additional cancer-specific biomarkers (TTF-1, GATA3, PAX8, calretinin, etc) to provide more cancer subtyping information. Interestingly, 1 patient in our cohort (patient 13) was diagnosed with mesothelioma; however, the tumor cells exhibited positive EpCAM staining in our ETC assay. A prior ipsilateral effusion also showed strong, diffuse, membranous MOC31 staining in addition to CK5/CK6, WT1, and calretinin positivity and harbored a *BAP1 M211fs* mutation. Given that positive EpCAM/MOC31 staining has been reported in 32% of patients with epithelioid mesothelioma,<sup>27,28</sup> we are interested in examining this patient further.

Another major advantage of our ETC-testing assay is to provide genetic profiling results using as few as 5 ETCs, which enabled us to examine disease-related mutations from a very specific group of cells. Different from the prevalent molecular testing method, which examines a mixed population of cells with either high or low tumor cellularity,<sup>29</sup> we used this ETC-profiling assay to analyze a much more homogenous groups of tumor cells. We were able to detect disease-driver mutations with 33% to 100% per-variant sensitivity compared with the clinical findings (Fig. 4F) and identified only germline variants in the patient sample with no malignancy. We acknowledge that the *EGFRL858R* mutation was not detected in our assay. We double-checked to confirm that coverage for the amplicons covering this locus was good. So, this observation could be a false negative result in our profiling assay, which requires us to test more ETC samples from this patient in the follow-up study. Our ETC profiling assay also reported additional mutations, including *RET* (*G691S*; 63%), *PIK3R1* (*M326I*; 48%), and *PTEN* (*C-9G*), which were filtered out as germline variants. These variants were also detected by the clinical molecular testing panel and were not reported because they were interpreted as germline or nonexonic. For future directions, we seek to collect more ETC samples and incorporate parallel on-slide germline controls for each patient to perform additional sequencing. If we can gain access to the tumor DNA used for the clinical sequencing, we will further perform parallel library preparation and sequencing of these clinical materials using our OncoZoom panel to compare with our ETC profiling

results. Last but not least, we are motivated to isolate more small clusters and large clusters of ETCs from any given patient to perform molecular profiling on different tumor cell groups, which we expect to reveal information about tumor heterogeneity.

In conclusion, we have developed a robust ETC identification assay that is able to identify rare carcinoma cells with high sensitivity and specificity from TP slides. We also isolated these confirmed ETCs and established a molecular profiling assay using 5 tumor cells. Next, we plan to expand these assays further by incorporating additional immunohistochemical markers and testing different sample types (peritoneal effusion, pericardial effusion, cerebrospinal fluid, urine, saliva, etc). We would expect that these assays may also apply to other material, such as fine-needle aspiration slides or histologic sections of cell blocks or surgical pathology specimens. Incorporation of this novel multiplexed immunofluorescent staining-based tumor cell characterization technology into pathology practice will expand and improve our clinical capabilities, enabling us to provide more using less for our patients and their treating clinicians.

#### FUNDING SUPPORT

No specific funding was reported.

#### CONFLICT OF INTEREST DISCLOSURES

Nolan G. Ericson and Tad C. George are employees of RareCyte Inc. The remaining authors made no disclosures.

#### AUTHOR CONTRIBUTIONS

**Yili Zhu:** Conceptualization, methodology, data collection and analysis, writing—original draft, and writing—review and editing. **Grace M. Allard:** Data collection and analysis and writing—review and editing. **Nolan G. Ericson:** Supervision, next-generation sequencing data analysis and interpretation, and writing—review and editing. **Tad C. George:** Supervision and writing—review and editing. **Christian A. Kunder:** Supervision, patient profiling data analysis and interpretation, and writing—review and editing. **Alarice C. Lowe:** Conceptualization, supervision, resources, writing—original draft, and writing—review and editing.

#### REFERENCES

1. Ferreira MM, Ramani VC, Jeffrey SS. Circulating tumor cell technologies. *Mol Oncol.* 2016;10:374-394. doi:10.1016/j.molonc.2016.01.007
2. Torre M, Lee EQ, Chukwueke UN, Nayak L, Cibas ES, Lowe AC. Integration of rare cell capture technology into cytologic evaluation of cerebrospinal fluid specimens from patients with solid tumors and suspected leptomeningeal metastasis. *J Am Soc Cytopathol.* 2020;9:45-54. doi:10.1016/j.jasc.2019.09.001
3. Cristofanilli M, Budd GT, Ellis MJ, et al. Circulating tumor cells, disease progression, and survival in metastatic breast cancer. *N Engl J Med.* 2004;351:781-791. doi:10.1056/NEJMoa040766
4. Smerage JB, Barlow WE, Hortobagyi GN, et al. Circulating tumor cells and response to chemotherapy in metastatic breast cancer: SWOG S0500. *J Clin Oncol.* 2014;32:3483-3489. doi:10.1200/JCO.2014.56.2561
5. de Bono JS, Scher HI, Montgomery RB, et al. Circulating tumor cells predict survival benefit from treatment in metastatic castration-resistant prostate cancer. *Clin Cancer Res.* 2008;14:6302-6309. doi:10.1158/1078-0432.CCR-08-0872
6. Cohen SJ, Punt CJA, Iannotti N, et al. Relationship of circulating tumor cells to tumor response, progression-free survival, and overall survival in patients with metastatic colorectal cancer. *J Clin Oncol.* 2008;26:3213-3221. doi:10.1200/JCO.2007.15.8923
7. Miller MC, Doyle GV, Terstappen LWMM. Significance of circulating tumor cells detected by the CellSearch system in patients with metastatic breast colorectal and prostate cancer. *J Oncol.* 2010;2010:617421. doi:10.1155/2010/617421
8. Crowley E, Di Nicolantonio F, Loupakis F, Bardelli A. Liquid biopsy: monitoring cancer-genetics in the blood. *Nat Rev Clin Oncol.* 2013;10:472-484. doi:10.1038/nrclinonc.2013.110
9. Diaz LA, Bardelli A. Liquid biopsies: genotyping circulating tumor DNA. *J Clin Oncol.* 2014;32:579-586. doi:10.1200/JCO.2012.45.2011
10. Junqueira-Neto S, Batista IA, Costa JL, Melo SA. Liquid biopsy beyond circulating tumor cells and cell-free DNA. *Acta Cytol.* 2019;63:479-488. doi:10.1159/000493969
11. Hiley CT, Le Quesne J, Santis G, et al. Challenges in molecular testing in non-small-cell lung cancer patients with advanced disease. *Lancet.* 2016;388:1002-1011. doi:10.1016/S0140-6736(16)31340-X
12. Siravegna G, Marsoni S, Siena S, Bardelli A. Integrating liquid biopsies into the management of cancer. *Nat Rev Clin Oncol.* 2017;14:531-548. doi:10.1038/nrclinonc.2017.14
13. Lemjabbar-Alaoui H, Hassan OU, Yang YW, Buchanan P. Lung cancer: biology and treatment options. *Biochim Biophys Acta.* 2015;1856:189-210. doi:10.1016/j.bbcan.2015.08.002
14. Hirsch FR, Scagliotti GV, Mulshine JL, et al. Lung cancer: current therapies and new targeted treatments. *Lancet.* 2017;389:299-311. doi:10.1016/S0140-6736(16)30958-8
15. Duma N, Santana-Davila R, Molina JR. Non-small cell lung cancer: epidemiology, screening, diagnosis, and treatment. *Mayo Clin Proc.* 2019;94:1623-1640. doi:10.1016/j.mayocp.2019.01.013
16. Bradley JD, Paulus R, Komaki R, et al. Standard-dose versus high-dose conformal radiotherapy with concurrent and consolidation carboplatin plus paclitaxel with or without cetuximab for patients with stage IIIA or IIIB non-small-cell lung cancer (RTOG 0617): a randomised, two-by-two factorial phase 3 study. *Lancet Oncol.* 2015;16:187-199. doi:10.1016/S1470-2045(14)71207-0
17. Senan S, Brade A, Wang LH, et al. PROCLAIM: randomized phase III trial of pemetrexed-cisplatin or etoposide-cisplatin plus thoracic radiation therapy followed by consolidation chemotherapy in locally advanced nonsquamous non-small-cell lung cancer. *J Clin Oncol.* 2016;34:953-962. doi:10.1200/JCO.2015.64.8824
18. Feller-Kopman D, Light R. Pleural disease. *N Engl J Med.* 2018;378:740-751. doi:10.1056/NEJMra1403503
19. Arnold DT, De Fonseca D, Perry S, et al. Investigating unilateral pleural effusions: the role of cytology. *Eur Respir J.* 2018;52:1801254. doi:10.1183/13993003.01254-2018
20. Porcel JM. Diagnosis and characterization of malignant effusions through pleural fluid cytological examination. *Curr Opin Pulm Med.* 2019;25:362-368. doi:10.1097/MCP.0000000000000593
21. Roy-Chowdhuri S, Dacic S, Ghofrani M, et al. Collection and handling of thoracic small biopsy and cytology specimens for ancillary studies: guideline from the College of American Pathologists in collaboration with the American College of Chest Physicians, Association for

- Molecular Pathology, American Society of Cytopathology, American Thoracic Society, Pulmonary Pathology Society, Papanicolaou Society of Cytopathology, Society of Interventional Radiology, and Society of Thoracic Radiology. *Arch Pathol Lab Med.* 2020;144:933-958. doi:10.5858/arpa.2020-0119-CP
22. Kaldjian EP, Ramirez AB, Sun Y, et al. The RareCyte® platform for next-generation analysis of circulating tumor cells. *Cytometry A.* 2018;93:1220-1225. doi:10.1002/cyto.a.23619
  23. Campton DE, Ramirez AB, Nordberg JJ, et al. High-recovery visual identification and single-cell retrieval of circulating tumor cells for genomic analysis using a dual-technology platform integrated with automated immunofluorescence staining. *BMC Cancer.* 2015;15:360. doi:10.1186/s12885-015-1383-x
  24. Lai Z, Markovets A, Ahdesmaki M, et al. VarDict: a novel and versatile variant caller for next-generation sequencing in cancer research. *Nucleic Acids Res.* 2016;44:e108. doi:10.1093/nar/gkw227
  25. Tate JG, Bamford S, Jubb HC, et al. COSMIC: the Catalogue of Somatic Mutations in Cancer. *Nucleic Acids Res.* 2019;47(D1):D941-D947. doi:10.1093/nar/gky1015
  26. Pinto D, Chandra A, Crothers BA, Kurtycz DFI, Schmitt F. The international system for reporting serous fluid cytopathology—diagnostic categories and clinical management. *J Am Soc Cytopathol.* 2020;9:469-477. doi:10.1016/j.jasc.2020.05.015
  27. Naso JR, Churg A. Claudin-4 shows superior specificity for mesothelioma vs non-small-cell lung carcinoma compared with MOC-31 and Ber-EP4. *Hum Pathol.* 2020;100:10-14. doi:10.1016/j.humpath.2020.04.005
  28. Fels Elliott DR, Jones KD. Diagnosis of mesothelioma. *Surg Pathol Clin.* 2020;13:73-89. doi:10.1016/j.path.2019.10.001
  29. Gray PN, Dunlop CLM, Elliott AM. Not All next generation sequencing diagnostics are created equal: understanding the nuances of solid tumor assay design for somatic mutation detection. *Cancers (Basel).* 2015;7:1313-1332. doi:10.3390/cancers7030837